Author(s): Valagiannopoulos, Constantinos & Sihvola, Ari

Title: Improving the electrostatic field concentration in a negative-permittivity wedge with a grounded bowtie configuration.

Year: 2013

Version: Final published version

Please cite the original version:

Valagiannopoulos, Constantinos & Sihvola, Ari. 2013. Improving the electrostatic field concentration in a negative-permittivity wedge with a grounded bowtie configuration. Radio Science. Volume 48, Issue 3. P. 316 325. 1944-799X (printed). DOI: 10.1002/rds.20035.

RADIO SCIENCE, VOL. 48, 316–325, doi:10.1002/rds.20035, 2013

Improving the electrostatic field concentration in a negative-permittivity wedge with a grounded "bowtie" configuration

Constantinos A. Valagiannopoulos[1] and Ari Sihvola[1]

Received 24 September 2012; revised 19 March 2013; accepted 20 April 2013; published 19 June 2013.

[1] Two wedges, one made of negative-permittivity material (primary) and another of an ordinary dielectric (auxiliary/secondary), are posed nose-to-nose to form a "bowtie" configuration. This shape is very common and convenient for a number of real-world devices and constructions such as electron microscopes, optical superlenses, and nanotips. In all these structures, the efficient operation and functionality get strongly assisted by the increased electromagnetic power concentration in the vicinity of the edge. Such a field enhancement is attempted with proper choice of the characteristics of the dielectric wedge to increase the field intensity over the cross section of the metamaterial one. A slowly varying field assumption is adopted to formulate approximate solutions to similar structures (sharp and rounded corners). A quality factor has been defined based on the power carried by the supported modal waves, if they are excited by a suitable electric source, in the presence and in the absence of the auxiliary wedge. This quantity expresses the intensity enhancement that could be achieved and is represented in graphs with respect to the dielectric wedge parameters. The characteristics of the secondary component that lead to a maximization of the electric power into the primary one are identified and explained. In particular, periodic variations of the angular extent of the secondary wedge are observed, and the number of maxima is increased with the dielectric permittivity of the constituent material.

Citation: Valagiannopoulos, C. A. and A. Sihvola (2013), Improving the electrostatic field concentration in a negative-permittivity wedge with a grounded "bowtie" configuration, *Radio Sci.*, *48*, 316–325, doi:10.1002/rds.20035.

1. Introductory Comment

[2] Wedge configurations or structures of sharp or rounded corners are very commonly utilized in models of optical devices, electromagnetic designs, and technologies in the nanoscale. They have attracted considerable attention, and therefore, they have been both analyzed theoretically and implemented experimentally. From the early 1970s [*Dobrzynski and Maradudin*, 1972; *Davis*, 1976], the dispersion relation for a single dielectric corner was obtained, and the supported electrostatic edge modes were determined. On the other hand, the singular field developed along a sharp edge, under electrodynamic regime, has been investigated in *Valagiannopoulos* [2009] together with the smoothing influence of a protecting cover. Furthermore, numerous structures composed of penetrable or metallic edges and prisms with applications in nano-optics of surface plasmon polaritons have been thoroughly examined in the study [*Zayats et al.*, 2005]. The developed surface modes in several canonical geometries with rounded corner interfaces between two materials have been investigated in *Wallen et al.* [2008], and the accompanying curvature effect is observed in *Passian et al.* [2005]. Finally, the electrostatic eigenmodes in a hyperbolic wedge are analytically determined in *Boardman et al.* [1985].

[3] In order to increase the experimental effectiveness of a device composed of sharp or rounded dielectric corners, it is natural to aim at enhancing the field concentration in the vicinity of the edge with a number of methods. In particular, microelectromechanical probes have been assisted by an electrostatic actuator to decrease the gap width and reinforce the optical near-field intensity [*Iwami et al.*, 2006]. Moreover, strongly amplified electromagnetic fields at moderate distances from a silver/gold wedge have been reported in *Angulo et al.* [2011], by manipulating morphology and dielectric environment. In *Gramotnev et al.* [2007], it is also demonstrated that during plasmon nanofocusing in a V-shaped tapered gap, the local electric field experiences much higher concentration than the magnetic field. Similarly, a sharp metal wedge has been shown to achieve an efficient adiabatic nanofocusing on a dielectric

[1]Department of Radio Science and Engineering, School of Electrical Engineering, Aalto University, Helsinki, Finland.

Corresponding author: C. A. Valagiannopoulos, Department of Radio Science and Engineering, School of Electrical Engineering, Aalto University, PO Box 13000, FI-00076 AALTO, Helsinki, Finland. (konstantinos.valagiannopoulos@aalto.fi)

0048-6604/13/10.1002/rds.20035

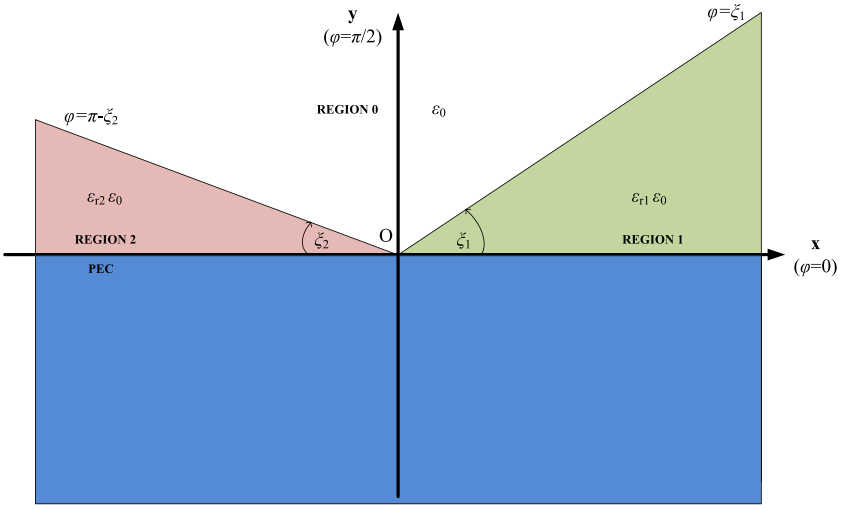

Figure 1. The "bowtie" wedge configuration. Two infinite dielectric wedges of different angular extents are backed by a perfectly conducting (PEC) plane and examined at the electrostatic regime.

substrate [*Vernon et al.*, 2007]. Finally, wedge configurations are routinely employed to imitate or model the functioning mechanism of nanotips [*Rockstuhl et al.*, 2009] or electron microscopes [*Zhang and Liu*, 2008], where increased field intensity in the vicinity of the dielectric corners is required for high scanning performances.

[4] In this work, we analyze, in the electrostatic regime, the possibility of increasing the electric field magnitude into a metamaterial (negative-permittivity) sharp wedge. It becomes feasible with help from another wedge of ordinary dielectric (permittivity larger than unity) which is posed against the metamaterial structure, by slightly touching its nose. Similar considerations have been thoroughly analyzed by prolific publishers in numerous works such as *Pendry et al*. [2012], *Aubry et al*. [2010], *Zeng et al*. [2011], and *Savage et al*. [2012]. The entire three-dimensional (3-D) configuration is grounded with an infinite perfectly conducting (PEC) plane which dictates a symmetry. We do not consider a specific excitation since our intention is to examine the internal (eigen)response of the configuration alone, isolated from external sources. In other words, to observe how the structure behaves naturally released from outward constraints. The electrostatic modes that lead to nontrivial field distribution are determined, and a quality factor expressing the intensity enhancement into the metamaterial wedge is defined.

[5] A simplified solution for the same problem is also obtained when the axial variation of the fields is not significant ("quasi-3D" case), by using the asymptotic expansion of the modified Bessel function. Under the same simplifying assumption, the corresponding hyperbolic wedge problem is considered, where the edges are rounded. The respective approximate solution is again derived by employing the related transformation formulas between the two coordinate systems (circular cylindrical and elliptic cylindrical). The same quality factor is defined in the aforementioned simplified cases. The variation of this indicative quantity with respect to the material and shape parameters are shown and discussed, revealing certain conclusions for every single of the regarded configurations.

2. Problem Statement

[6] Consider the structure depicted in Figure 1, where the used Cartesian (x, y, z) and cylindrical (ρ, ϕ, z) coordinate systems are also defined. Two infinite dielectric sharp wedges, backed by an infinite PEC plane ($y = 0$), are posed nose-to-nose, forming an asymmetric "bowtie" configuration. The wedge positioned at the rightmost region (region 1) has an angular extent of ξ_1 and is filled with a plasmonic substance of relative permittivity $\epsilon_{r1} < 0$. The left wedge (region 2) is of angle ξ_2 and its material has relative dielectric constant $\epsilon_{r2} > 1$. The entire structure is surrounded by vacuum (region 0), permittivity ϵ_0), and the problem is investigated under the electrostatic regime. We choose to study a configuration which is nonpenetrable across its lower half (PEC half-space $y < 0$), to restrict the value range of the azimuthal angle $\phi \in [0, \pi]$. In this way, no periodic solutions with respect to ϕ are required, and a physical consistency is retained.

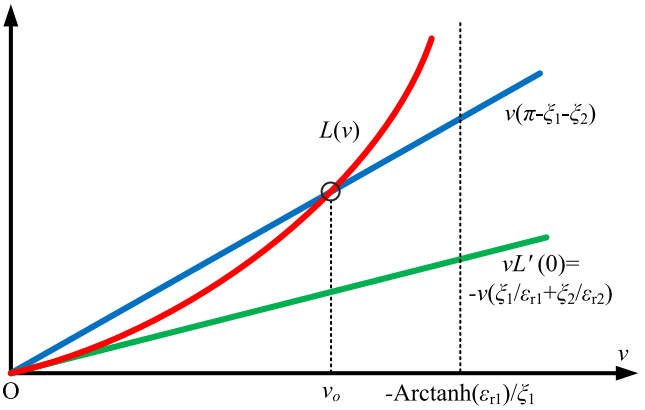

Figure 2. A symbolic typical graph of the left-hand side (LHS), the right-hand side (RHS) of the dispersion relation (11), and the tangent line of the LHS at the origin. The cross point (supported mode) and the vertical asymptote of the LHS are also shown.

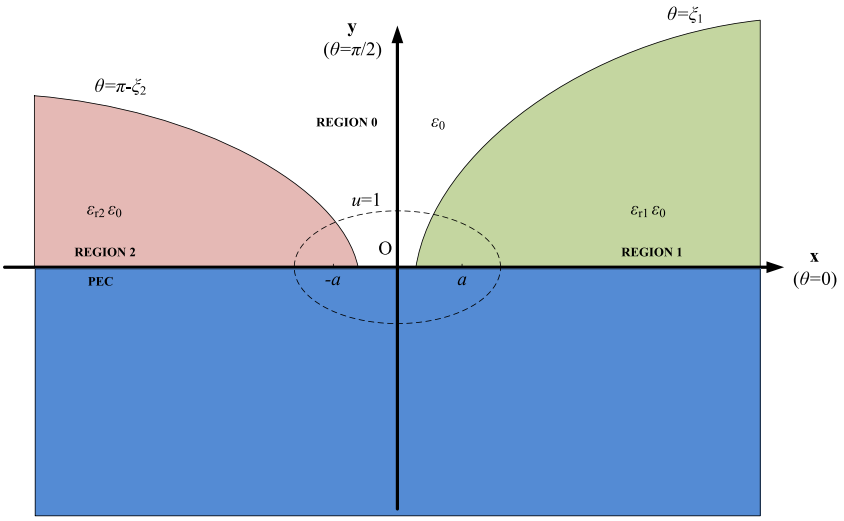

Figure 3. The hyperbolic "bowtie" configuration. Two infinite dielectric hyperbolic cylinders of different angular extents are backed by a perfectly conducting (PEC) plane and examined at the electrostatic regime.

[7] The scope of this work is to examine the effect of the second wedge (secondary, auxiliary component) on the field concentration into the first wedge (primary, main component) in the vicinity of the edge. We are going to evaluate the modes of the described structure, namely the permissible electric field distributions over the cross sections of the objects regardless of the excitation type. In addition, we will examine certain slightly different considerations either with respect to the field variation or concerning the shape of the boundaries.

3. 3-D Exact Solution

3.1. General Formulas

[8] In each region of the regarded configuration, the electrostatic potential $\Phi(\rho, \phi, z)$ obeys the Laplace equation:

$$\nabla^2 \Phi(\rho, \phi, z) = 0. \tag{1}$$

If the separation of variables is applied: $\Phi(\rho, \phi, z) = f_\rho(\rho) f_\phi(\phi) f_z(z)$, it is directly found that the partial solutions possess the general forms:

$$f_\rho(\rho) = A_\rho I_{j\nu}(\mu\rho) + B_\rho K_{j\nu}(\mu\rho), \tag{2}$$

$$f_\phi(\phi) = A_\phi \cosh(\nu\phi) + B_\phi \sinh(\nu\phi), \tag{3}$$

$$f_z(z) = A_z \cos(\mu z) + B_z \sin(\mu z), \tag{4}$$

where I, K are the modified Bessel functions, j is the imaginary unit, and $\mu, \nu \in \mathbb{C}$. It should be remarked that we make the assumption that the solution is written in separable form, which does not mean that other, more complicated, potential distributions cannot exist. Therefore, whatever formulation hereinafter is called as "not acceptable" or "non supported," implies that it is not compatible with the separation-of-variables adopted approach; not that it is unnatural or physically impossible to get developed. Furthermore, due to the fact that only the fields are dependent on z coordinate contrary to the configuration, the term "three-dimensional" could be replaced by the more descriptive one "extruded two-dimensional."

[9] In order to avoid exponentially increasing solutions along the **z** axis, we restrict the complex spectral parameter μ to real values: $\mu \in \mathbb{R}$. In the same way, the solution $I_{j\nu}(\mu\rho)$ is rejected ($A_\rho = 0$), since this function is exponentially increasing for large ρ regardless of the value $\nu \in \mathbb{C}$. Furthermore, the imaginary part of ν should be zero ($\Im[\nu] = 0$); otherwise, the modified Bessel function becomes singular at the origin $(x, y) = (0, 0)$: $|K_{j\nu}(0)| \to +\infty$. Finally, ν should be positive since the same function increases unboundedly for $\rho \to +\infty$ (and $\mu < 0$). The range of the out-of-plane wave number μ cannot be confined further since the function $K_{j\nu}(\tau)$ is not even or odd with respect to τ.

[10] Due to the presence of the infinite plane, the tangential components (**x**, **z**) of the electric field into regions 1 and 2 should be zero along $y = 0$ (Figure 1). Therefore, only one of the two linearly independent azimuthal solutions would be present in the expressions corresponding to regions 1 and 2. On the other hand, the two axial, z-dependent functions are present in all the regions and form two solution sets: one even and one odd with respect to **z** axis. These two sets are not coupled each other due to the matching of the fields along the axial direction.

3.2. Dispersion Equation

[11] The explicit formulas for the electrostatic potential in each region (0, 1, and 2) are given by:

$$\Phi_0(\rho, \phi, z) = K_{j\nu}(\mu\rho)\,[A_0 \cosh(\nu(\phi - \gamma)) + B_0 \sinh(\nu(\phi - \gamma))] \begin{Bmatrix} \cos(\mu z) \\ \sin(\mu z) \end{Bmatrix}, \tag{5}$$

$$\Phi_1(\rho, \phi, z) = K_{j\nu}(\mu\rho) B_1 \sinh(\nu\phi) \begin{Bmatrix} \cos(\mu z) \\ \sin(\mu z) \end{Bmatrix}, \tag{6}$$

$$\Phi_2(\rho, \phi, z) = K_{j\nu}(\mu\rho) B_2 \sinh(\nu(\phi - \pi)) \begin{Bmatrix} \cos(\mu z) \\ \sin(\mu z) \end{Bmatrix}, \tag{7}$$

where $\gamma = \frac{\pi - \xi_2 + \xi_1}{2}$ is the azimuthal angle that divides region 0 into two symmetric subregions. The necessary boundary

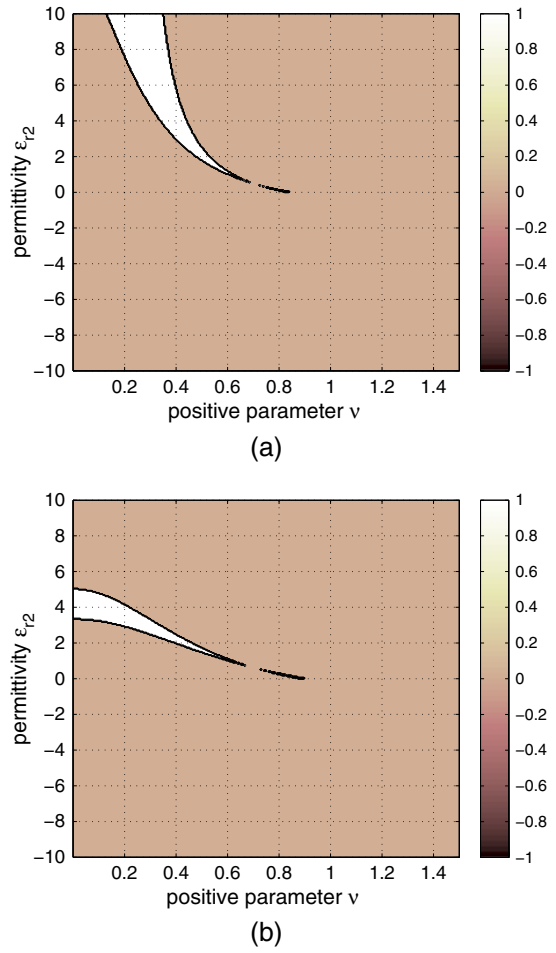

Figure 4. The contour plot of the quantized dispersion equation (one if it is fulfilled, zero if not) with respect to the positive parameter ν and the permittivity of the secondary wedge ϵ_{r2} for: (a) $\xi_2 = 45°$ and (b) $\xi_2 = 60°$. Plot parameters: $\epsilon_{r1} = -0.5$, $\xi_1 = 45°$.

conditions along the surfaces $\phi = \xi_1, (\pi - \xi_2)$ are shown below:

$$\Phi_0|_{\phi=\xi_1} = \Phi_1|_{\phi=\xi_1} \quad , \quad \Phi_0|_{\phi=\pi-\xi_2} = \Phi_2|_{\phi=\pi-\xi_2} \, , \tag{8}$$

$$\left.\frac{\partial \Phi_0}{\partial \phi}\right|_{\phi=\xi_1} = \epsilon_{r1} \left.\frac{\partial \Phi_1}{\partial \phi}\right|_{\phi=\xi_1} \quad , \quad \left.\frac{\partial \Phi_0}{\partial \phi}\right|_{\phi=\pi-\xi_2} = \epsilon_{r2} \left.\frac{\partial \Phi_2}{\partial \phi}\right|_{\phi=\pi-\xi_2} . \tag{9}$$

After imposing them on the formulas (5)–(7), one obtains the following equation:

$$\tanh(\nu\xi_1) = -\epsilon_{r1} \frac{\epsilon_{r2} \tanh(\nu(\pi - \xi_1 - \xi_2)) + \tanh(\nu(\xi_2))}{\epsilon_{r2} + \tanh(\nu(\pi - \xi_1 - \xi_2)) \tanh(\nu(\xi_2))}. \tag{10}$$

The solutions of this equation with respect to $\nu > 0$, corresponds to the permissible field distributions into the entire configuration. Therefore, this is the dispersion equation and should be verified in order for the electric field to exist.

[12] After employing well-known properties of the hyperbolic functions, the dispersion relation is written as:

$$L(\nu) = -\text{Arctanh}\left[\frac{\tanh(\nu\xi_1)}{\epsilon_{r1}}\right] - \text{Arctanh}\left[\frac{\tanh(\nu\xi_2)}{\epsilon_{r2}}\right] = \nu(\pi - \xi_1 - \xi_2). \tag{11}$$

It should be remarked that for $\epsilon_{r1}, \epsilon_{r2} \to \infty$, the solution to that equation is $\nu = 0$ which is trivial and corresponds to null (zero) fields. Such a result is compatible with the standard Schwarz-Christoffel solutions [*Smythe*, 1950] of a pair of a ground wedges touching each other. The same expression (11) is obtained if one changes the parameter ξ_1 by ξ_2 and vice versa, a feature that is justified by the symmetry of the structure. The right-hand side (RHS) of the equation above is an upward sloping straight line with always positive sign since $\xi_1 + \xi_2 < \pi$ from the definition of the configuration. Note that the left-hand side (LHS) $L(\nu)$ tends to complex infinity for $-1 < \epsilon_{r1} < 0$, if we take for granted that the second sharp wedge is filled with an ordinary dielectric material $\epsilon_{r2} > 1$. Under these conditions, the function $L(\nu)$ starts from zero and takes unboundedly large positive values at this $\nu > 0$ dictated by the equation: $\tanh(\nu\xi_1) = -\epsilon_{r1}$. For $\nu > -\frac{\text{Arctanh}(\epsilon_{r1})}{\xi_1}$, the LHS becomes complex, and thus, no solution for (11) is detected. The derivative of the LHS is given by:

$$L'(\nu) = -\frac{\epsilon_{r1}\xi_1}{1 + \left(\epsilon_{r1}^2 - 1\right)\cosh^2(\nu\xi_1)} - \frac{\epsilon_{r2}\xi_2}{1 + \left(\epsilon_{r2}^2 - 1\right)\cosh^2(\nu\xi_2)}. \tag{12}$$

It should be stressed that for the all the considered cases, the function $L(\nu)$ and its derivative $L'(\nu)$ preserve their (positive) sign for every $\nu > 0$.

[13] A typical variation of the quantities appeared in the field existence condition is shown in Figure 2. The red curve corresponds to the function $L(\nu)$, the blue curve concerns the linear RHS $\nu(\pi - \xi_1 - \xi_2)$, and the green curve is the tangent of $L(\nu)$ at $\nu = 0$. It is apparent that a positive solution $\nu = \nu_o > 0$ (apart from the trivial $\nu = 0$ which leads to all-zero fields) for (11), is feasible when the (positive) derivative of the LHS $L(\nu)$ at $\nu = 0$ is smaller than the (always positive) slope of the linear RHS $(\pi - \xi_1 - \xi_2)$. In other words, the necessary inequality constraint is written as follows:

$$0 < L'(0) < \pi - \xi_1 - \xi_2 \Rightarrow \xi_1 + \xi_2 < \left(1 - \frac{1}{\epsilon_{r1}}\right)\xi_1 + \left(1 - \frac{1}{\epsilon_{r2}}\right)\xi_2 < \pi. \tag{13}$$

Note that the analysis above is valid regardless of the z-dependence of (5)–(7). Our choice to confine the permittivity of the primary component within the range $\epsilon_{r1} \in (-1, 0)$ is compatible with the results for the azimuthally odd modes of a single wedge [*Wallen et al.*, 2008].

3.3. Quality Factor

[14] Assume that the case we analyze requires a certain positive solution $\nu = \nu_o$. Let us compute the electric field into region 1 from the well-known formula: $\mathbf{E}_1(\rho, \phi, z) = -\nabla\Phi_1(\rho, \phi, z)$. The components in cylindrical coordinates are given by:

$$E_{1\rho}^{(\nu_o)}(\rho, \phi, z) = -f_\rho'(\rho) B_1 \sinh(\nu_o\phi) \begin{Bmatrix} \cos(\mu z) \\ \sin(\mu z) \end{Bmatrix}, \tag{14}$$

$$E_{1\phi}^{(\nu_o)}(\rho, \phi, z) = -\nu_o \frac{f_\rho(\rho)}{\rho} B_1 \cosh(\nu_o\phi) \begin{Bmatrix} \cos(\mu z) \\ \sin(\mu z) \end{Bmatrix}, \tag{15}$$

$$E_{1z}^{(\nu_o)}(\rho, \phi, z) = -\mu f_\rho(\rho) B_1 \sinh(\nu_o\phi) \begin{Bmatrix} -\sin(\mu z) \\ \cos(\mu z) \end{Bmatrix}, \tag{16}$$

where $f_\rho(\rho) = K_{j\nu_o}(\mu\rho)$ in this case. Due to the lack of sources in the regarded problem, we determine the eigensolutions of it; on the contrary, a unique solution can be derived

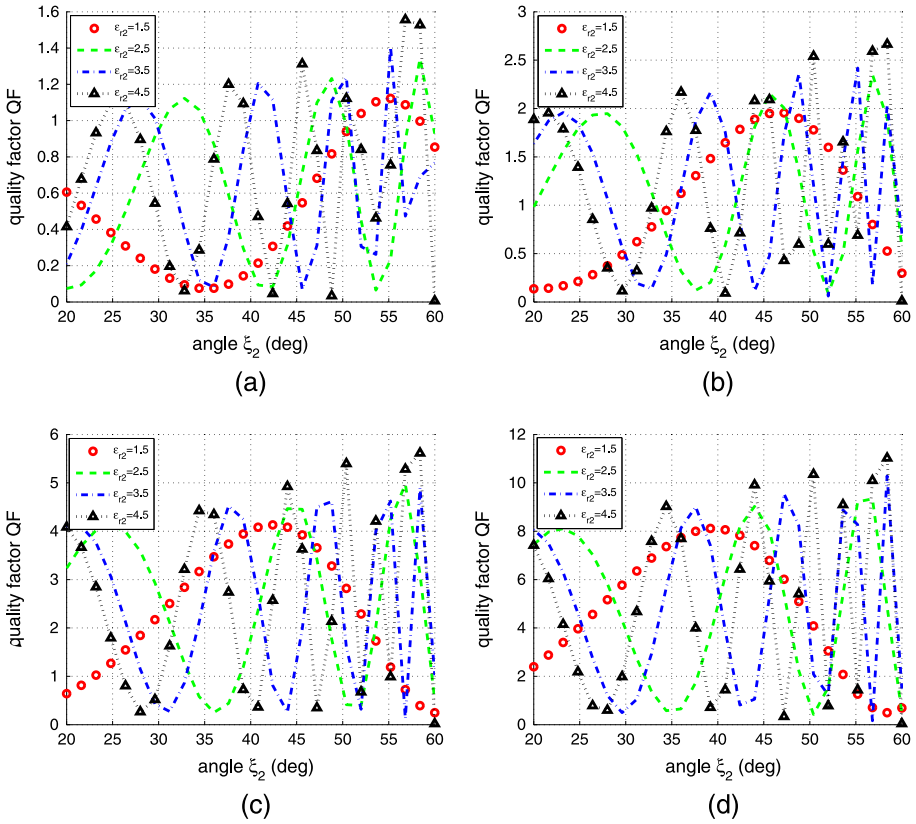

Figure 5. The quality factor $\mathcal{QF}$ as function of the angle ξ_2 for several permittivities ϵ_{r2} with use of the exact circular cylindrical solution for: (a) $\mu = 0.1$ rad/m, (b) $\mu = 0.4$ rad/m, (c) $\mu = 0.7$ rad/m, and (d) $\mu = 1$ rad/m. Plot parameters: $\epsilon_{r1} = -0.5$, $\xi_1 = 45°$, $R = 1$ m, $h = 1$ m, even case.

only under a specific, well-defined excitation. In particular, we find the family of solutions for the electrostatic potential and the electric field that formulate physically consistent concepts. This uncertainty is expressed through the arbitrary real (proportional) constant B_1 appeared above when finding the electric field for the first sharp wedge. We assume that this parameter takes a unitary value $B_1 = 1$, and thus, the effect of the surrounding configuration (second wedge, vacuum background, PEC plane) is solely expressed through the solution $\nu = \nu_o$ of (11).

[15] To estimate the influence of the second component on the field concentration of the first wedge, one can define the following power ratio developed into the three-dimensional sector: $\{0 < \rho < R, 0 < \phi < \xi_1, -h < z < h\}$.

$$\mathcal{QF} = \frac{\int_{-h}^{h}\int_{0}^{\xi_1}\int_{0}^{R}\left[|E_{1\rho}^{(\nu_o)}|^2 + |E_{1\phi}^{(\nu_o)}|^2 + |E_{1z}^{(\nu_o)}|^2\right]\rho \mathrm{d}\rho\mathrm{d}\phi\mathrm{d}z}{\int_{-h}^{h}\int_{0}^{\xi_1}\int_{0}^{R}\left[|E_{1\rho}^{(\nu'_o)}|^2 + |E_{1\phi}^{(\nu'_o)}|^2 + |E_{1z}^{(\nu'_o)}|^2\right]\rho \mathrm{d}\rho\mathrm{d}\phi\mathrm{d}z}, \quad (17)$$

where ν'_o is the solution to (11) for $\epsilon_{r2} = 1$ and $\xi_2 = 0$ which corresponds to the case of an absent auxiliary wedge. Note that the dependence of the field components on the observation point (ρ, ϕ, z) has been dropped for brevity. In other words, this quality factor indicator $\mathcal{QF}$ shows how much the electric field close to the origin has been amplified, in the presence of the secondary sharp wedge component. If it is larger than unity ($\mathcal{QF} > 1$), then the design structure serves well its electrostatic field enhancement purpose. It should be mentioned that the point $\rho = 0$ is excluded from the integrations since the integrand functions exhibit nonintegrable singularity: $|E_{1\rho}|^2, |E_{1\phi}|^2 = O\left(1/\rho^2\right), \rho \to 0$. In particular, we replace the lower limit with a small positive quantity $r \to 0$; however, it does not play a significant role since the same singularity is dropped from both the numerator and the denominator of (17).

4. "Quasi–3D" Approximate Solutions

4.1. Circular Cylindrical Coordinates

[16] Based on the complete solution for the 3-D structure of Figure 1 described above, it would be interesting to examine its behavior when the variation along **z** axis is not significant. In other words, we are investigating a "quasi-3D" situation which corresponds to the case that the parameter μ is small: $\mu \to 0$. The ρ-dependent solution for a pure 2-D case ($\Phi(\rho, \phi) = f_\rho(\rho) f_\phi(\phi)$) is given by *Vinogradov and Liu* [2001]:

$$f_\rho(\rho) = A_\rho \cos(\nu \log \rho) + B_\rho \sin(\nu \log \rho), \quad (18)$$

while $f_\phi(\phi)$ possesses the same expression (3) as in the 3-D case. The corresponding radial formula in the 3-D problem

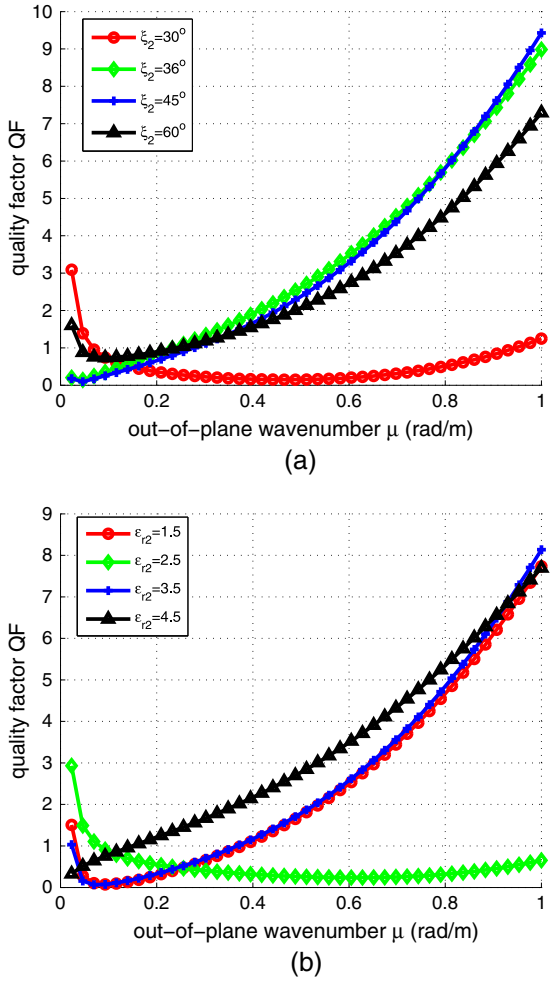

Figure 6. The quality factor $\mathcal{QF}$ as function of the out-of-plane wave number μ for: (a) several angles ξ_2 ($\epsilon_{r2} = 4$) and (b) several permittivities ϵ_{r2} ($\xi_2 = 36°$). Plot parameters: $\epsilon_{r1} = -0.5$, $\xi_1 = 45°$, $R = 1$ m, $h = 1$ m, even case.

equals to $K_{j\nu}(\mu\rho)$ and takes the following limiting form for small arguments (based on *Abramowitz and Stegun* [1970]):

$$f_\rho(\rho) \cong K_{j\nu}(\mu\rho) \cong \Re[\Gamma(j\nu)]\cos\left[\nu\log\left(\frac{\mu\rho}{2}\right)\right] + \Im[\Gamma(j\nu)]\sin\left[\nu\log\left(\frac{\mu\rho}{2}\right)\right] \quad , \quad \mu \to 0. \tag{19}$$

If we keep the same z-dependence $f_z(z)$ dictated by (4), then the Laplacian of function of the electromagnetic potential $\Phi(\rho,\phi,z) = f_\rho(\rho)f_\phi(\phi)f_z(z)$ is given by:

$$\nabla^2\Phi(\rho,\phi,z) \cong -\mu^2 f_\rho(\rho)\left[A_\phi\cosh(\nu\phi) + B_\phi\sinh(\nu\phi)\right] \cdot \left[A_z\cos(\mu z) + B_z\sin(\mu z)\right] \quad , \quad \mu \to 0. \tag{20}$$

It is obvious that for the "quasi-3D" case ($0 \neq \mu \to 0$), the aforementioned expression $\Phi(\rho,\phi,z)$ approximately obeys the Laplace differential equation. It should be stressed that the only difference with the set of solutions (2)–(4) is in the radial function $f_\rho(\rho)$ since the other dependencies are the same as in the 3-D case: $\{f_\phi(\phi) = A_\phi\cosh(\nu\phi) + B_\phi\sinh(\nu\phi), f_z(z) = A_z\cos(\mu z) + B_z\sin(\mu z)\}$. Accordingly, the dispersion equation (11) is also valid for the considered case because the ρ-dependent function $f_\rho(\rho)$ is common for all the considered areas and is factored out. Therefore, the formulas (14)–(16) determining the electric field into region 1 are correct (with $f_\rho(\rho)$ as given by (19)) for the investigated cylindrical "quasi-3D" approach; the same happens for the definition (17) of the quality factor $\mathcal{QF}$.

4.2. Elliptic Cylindrical Coordinates

[17] Under the same assumption of slowly varying fields with respect to z coordinate, one can solve another interesting configuration with slightly different characteristics. In particular, we consider the elliptic cylindrical coordinate system (u,θ,z) with focal distance a [*Hassani*, 2000] and the physical configuration depicted in Figure 3. It is similar to that of Figure 1 with the difference that the two dielectric regions (1 and 2) have hyperbolic and not planar boundaries; accordingly, a small gap exists in-between the two wedge noses. The angular values defining the two boundaries are the same as in the cylindrical problem: $\theta = \xi_1$ and $\theta = \pi - \xi_2$. Note that the elliptic cylindrical coordinates (u,θ,z) are related to the Cartesian ones (x,y,z) by the following:

$$x = a\cosh u\cos\theta, \tag{21}$$

$$y = a\sinh u\sin\theta, \tag{22}$$

where $u \geq 0$ and $\theta \in [0, 2\pi)$. The unknown potential function is again defined in separable form: $\Phi(u,\theta,z) = f_u(u)f_\theta(\theta)f_z(z)$. In order to find an approximate solution to this new boundary value problem, we consider points relatively far from the origin ($u >> 1$) where the two coordinate systems (u,θ,z) and (ρ,ϕ,z) are identical. In particular,

$$x \cong \frac{a}{2}e^u\cos\theta \quad , \quad u >> 1, \tag{23}$$

$$y \cong \frac{a}{2}e^u\sin\theta \quad , \quad u >> 1, \tag{24}$$

which means that: $\tan\phi = \frac{y}{x} \cong \tan\theta \Rightarrow \theta \cong \phi$, $u >> 1$. That is why, the hyperbolic angles of the dielectric volumes ($\theta = \xi_1, \pi - \xi_2$) were kept equal to those in the circular cylindrical case. As far as the connection between the parameters u and ρ is concerned, we have the relations:

$$\rho \cong \frac{a}{2}e^u \Leftrightarrow u \cong \log\left(\frac{2\rho}{a}\right) \quad , \quad u >> 1, \tag{25}$$

since $\rho^2 = x^2 + y^2 \cong \frac{a^2}{4}e^{2u}$, $u >> 1$. By substituting (25) to (19), the following expression for $f_u(u)$ is obtained:

$$f_u(u) \cong \Re[\Gamma(j\nu)]\cos\left[\nu u - \nu\log\left(\frac{4}{\mu a}\right)\right] + \Im[\Gamma(j\nu)]\sin\left[\nu u - \nu\log\left(\frac{4}{\mu a}\right)\right] \quad , \quad \mu \to 0. \tag{26}$$

[18] Given the fact the u-dependent solution set of the considered 2-D problem is the following: $\{\cos(\nu u), \sin(\nu u)\}$, the aforementioned expression is acceptable in terms of the satisfaction of the Laplace differential equation in the 2-D elliptic cylindrical coordinate system. Therefore, we have determined the correct formula which is satisfactorily accurate not only for $u >> 1$ but for every $u > 0$. By retaining the same θ-dependence ($f_\theta(\tau) = f_\phi(\tau)$) and z-dependent

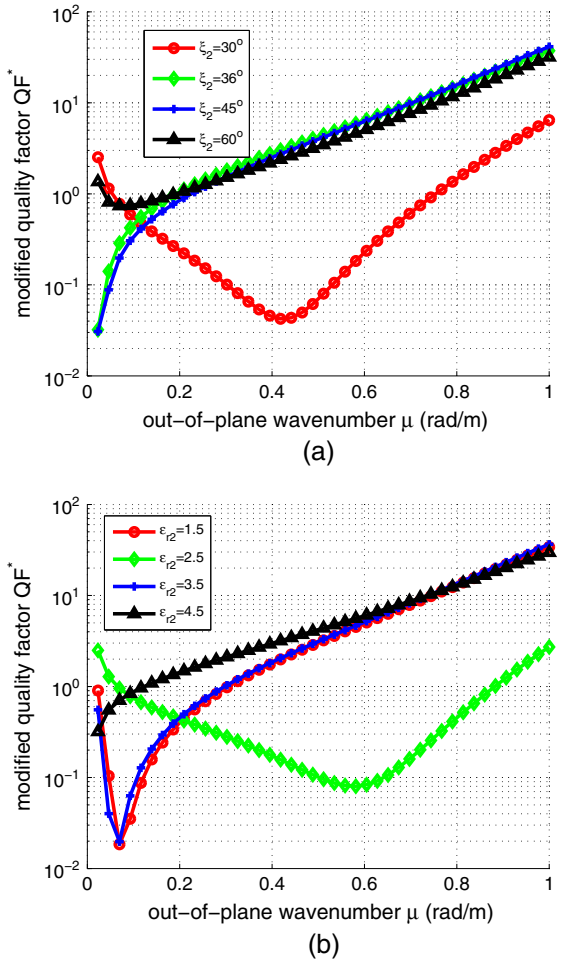

Figure 7. The modified quality factor $\mathcal{QF}^*$ as function of the out-of-plane wave number μ for: (a) several angles ξ_2 ($\epsilon_{r2} = 4$) and (b) several permittivities ϵ_{r2} ($\xi_2 = 36°$). Plot parameters: $\epsilon_{r1} = -0.5$, $\xi_1 = 45°$, $R = 1$ m, $h = 1$ m, even case.

functions as in (3) and (4), respectively, the Laplacian of function of the electrostatic potential $\Phi(u,\theta,z)$ is given by:

$$\nabla^2\Phi(u,\theta,z) \cong -\mu^2 f_u(u)\,[A_\theta \cosh(\nu\theta) + B_\theta \sinh(\nu\theta)] \cdot [A_z \cos(\mu z) + B_z \sin(\mu z)] \;,\; \mu \to 0. \tag{27}$$

Again, the function $\Phi(u,\theta,z)$ satisfies the Laplace equation for $\mu \to 0$. The three components of the electric field into region 1 are found by proper application of the gradient operator [*Morse and Feshbach*, 1953], on the electrostatic potential function ($\mathbf{E}_1(u,\theta,z) = -\nabla\Phi_1(u,\theta,z)$) as follows:

$$E_{1u}^{(\nu_o)}(u,\theta,z) = -\frac{f_u'(u)}{a\sqrt{\sinh^2 u + \sin^2\theta}} B_1 \sinh(\nu_o\theta) \begin{Bmatrix} \cos(\mu z) \\ \sin(\mu z) \end{Bmatrix}, \tag{28}$$

$$E_{1\theta}^{(\nu_o)}(u,\theta,z) = -\nu_o \frac{f_u(u)}{a\sqrt{\sinh^2 u + \sin^2\theta}} B_1 \cosh(\nu_o\theta) \begin{Bmatrix} \cos(\mu z) \\ \sin(\mu z) \end{Bmatrix}, \tag{29}$$

$$E_{1z}^{(\nu_o)}(u,\theta,z) = -\mu f_u(u) B_1 \sinh(\nu_o\theta) \begin{Bmatrix} -\sin(\mu z) \\ \cos(\mu z) \end{Bmatrix}. \tag{30}$$

It is noteworthy that the dispersion relation (11), possessing the solution $\nu = \nu_o > 0$, covers also the analyzed hyperbolic wedge configuration. This peculiar feature is attributed to the fact that the solution set with respect to the circular cylindrical variable ϕ: $\{\cosh(\nu\phi), \sinh(\nu\phi)\}$, is identical to that of the elliptic cylindrical variable θ: $\{\cosh(\nu\theta), \sinh(\nu\theta)\}$. In this sense, the quality factor $\mathcal{QF}$ is expressed in the adopted coordinate system as follows:

$$\mathcal{QF} = \frac{\int_{-h}^{h}\int_0^{\xi_1}\int_0^{\log\left(\frac{2R}{a}\right)} \left[|E_{1u}^{(\nu_o)}|^2 + |E_{1\theta}^{(\nu_o)}|^2 + |E_{1z}^{(\nu_o)}|^2\right](\sinh^2 u + \sin^2\theta)\,\mathrm{d}u\mathrm{d}\theta\mathrm{d}z}{\int_{-h}^{h}\int_0^{\xi_1}\int_0^{\log\left(\frac{2R}{a}\right)} \left[|E_{1u}^{(\nu_o')}|^2 + |E_{1\theta}^{(\nu_o')}|^2 + |E_{1z}^{(\nu_o')}|^2\right](\sinh^2 u + \sin^2\theta)\,\mathrm{d}u\mathrm{d}\theta\mathrm{d}z}. \tag{31}$$

Note that the differential volume element of the elliptic cylindrical coordinates (u,θ,z) with focal distance a, is defined as: $\mathrm{d}V = a^2(\sinh^2 u + \sin^2\theta)\,\mathrm{d}u\mathrm{d}\theta\mathrm{d}z$. The integral with respect to u has an upper limit equal to $\log\left(\frac{2R}{a}\right)$, in order to consider an approximately equal area as this in (17), with use of (25). The point $(u,\theta) = (0,0)$ is not singular since the square root quantities at the denominators are neutralized by the identical ones incorporated in dV.

5. Numerical Results

5.1. Parameter Ranges

[19] As remarked previously, the primary wedge is filled with metamaterials of negative permittivities within the limits: $-1 < \epsilon_{r1} < 0$; therefore, we will keep fix the dielectric constant equal to the average value: $\epsilon_{r1} = -0.5$, to understand better the influence of the secondary structure. This auxiliary wedge is made of a dielectric with dielectric constant: $1 < \epsilon_{r2} < 5$. The latter choice of the common dielectric material for the secondary wedge is made based on our intention to employ an ordinary substance to construct the auxiliary component instead of materials with special or exotic properties. As far as the angular extents are concerned, they are obeying the inequality: $0 < \xi_1, \xi_2 < \pi/2$; while in most examples, we take $\xi_1 = \pi/4$ for the reason stated above. It is notable that negative permittivities ϵ_{r2} for the secondary wedge do not anyway lead to supported separable modes by the background structure with $\epsilon_{r1} = -0.5$ and $\xi_1 = \pi/4$ since a positive ν satisfying the dispersion equation (10) does not exist in most cases. In Figure 4, we show the contour plots of a quantity indicating those combinations of (ν, ϵ_{r2}) leading to a supported mode-solution to (10) under the separation-of-variables assumption. In particular, the represented quantity is defined as follows:

$$S(\nu,\epsilon_{r2}) = \begin{cases} 1 & ,|L(\nu) - \nu(\pi - \xi_1 - \xi_2)| \le 0.02 \\ 0 & ,|L(\nu) - \nu(\pi - \xi_1 - \xi_2)| > 0.02 \end{cases}. \tag{32}$$

Therefore, the white regions (value 1) in the depicted contour plots, correspond to permissible combinations of (ν, ϵ_{r2}); on the contrary, the dark regions (value 0) indicate those cases that no mode is supported in the sense stated above. By inspection of the graphs in Figure 4a ($\xi_2 = \pi/4$) and in Figure 4b ($\xi_2 = \pi/3$), it is directly derived that no $\nu > 0$ constitutes a solution for (10) when $\epsilon_{r2} < 0$.

[20] The out-of-plane wave number μ should be real ($\mu \in \mathbb{R}$), but we confine ourselves to positive values 0.1 rad/m< μ <1 rad/m due to symmetry with respect to **z** axis. Naturally, in the "quasi-3D" cases, we select an even

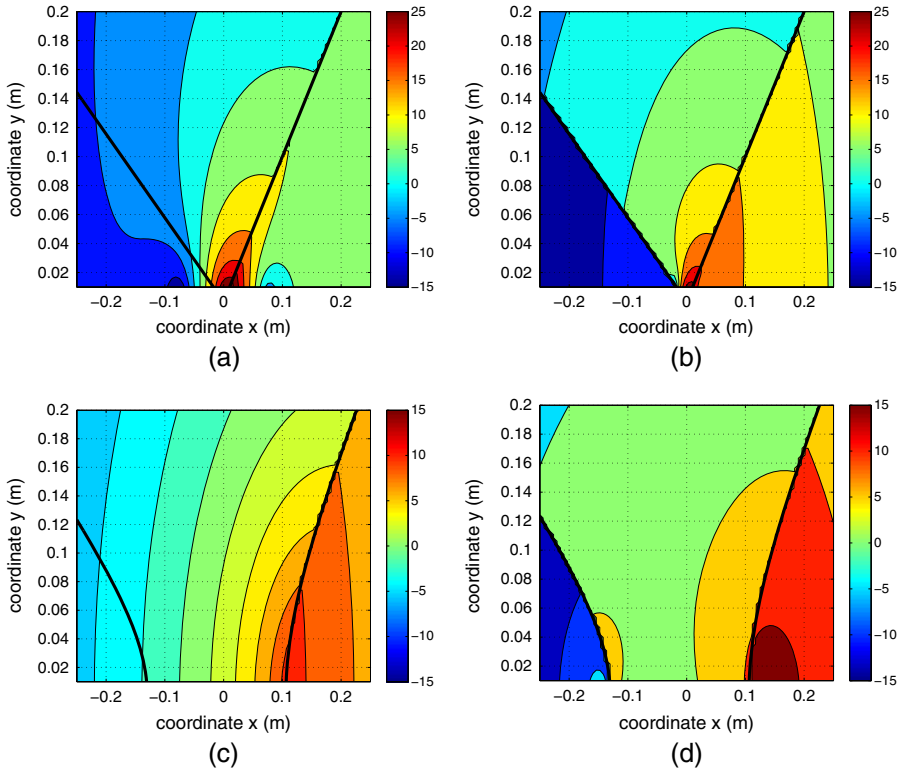

Figure 8. The magnitude of the electric field $|\mathbf{E}|$ represented in contour plot with respect to the geometrical coordinates with use of: (a) the approximate circular cylindrical solution ($\epsilon_{r2} = 1$), (b) the approximate circular cylindrical solution ($\epsilon_{r2} = 5$), (c) the approximate elliptic cylindrical solution ($\epsilon_{r2} = 1$, $a = 0.15$ m), and (d) the approximate elliptic cylindrical solution ($\epsilon_{r2} = 5$, $a = 0.15$ m). Plot parameters: $\mu = 0.1$ rad/m, $\xi_1 = 45°$, $\xi_2 = 30°$, $z = 0$ m, even case.

smaller $\mu \to 0$, more specifically: $0 < \mu < 0.1$. In the case of the hyperbolic wedges, the distance a varies from infinitesimal $a = 0.0001$ m to a substantial $a = 1$ m, which is unnatural but necessary for identifying the effect of the edge rounding. The reference radius R which is used in evaluating the quality factor $\mathcal{QF}$ is chosen small too, in order to observe the behavior of the field in the vicinity of the (sharp or rounded) edge. The axial length $2h$ can be selected arbitrarily since it does not affect significantly the variation of our sole output quantity which is the quality factor $\mathcal{QF}$. It has been also checked that the choice of the z-dependence (even waves with $\cos(\mu z)$ or odd waves with $\sin(\mu z)$) plays no role in the value of $\mathcal{QF}$ due to the relative nature of the evaluated quantity. Needless to say that for all the considered cases, the dispersion equation (10) in the presence and in the absence of the auxiliary wedge possesses acceptable solutions $\nu_o > 0$ and $\nu_o' > 0$ (in separable form), respectively.

[21] A sensible criticism for the definition of $\mathcal{QF}$ would be based on the fact that the field quantities are not the unique solution to a given boundary value problem under a certain excitation but simply modal forms supported by the structure. Our response on this remark is that the background field or the source could be chosen suitably to excite a specific mode. In other words, if a large field enhancement is observed for a specific combination of input parameters, then similarly increased power concentration would be noticed when comparing actual field quantities for a properly selected excitation. This argument is further reinforced by the feature that, in our configuration, one single mode ($\nu = \nu_o, \nu_o'$) is supported by the given structure. Therefore, part of the background field power (excitation field) would inevitably excite the single mode both in the case of an absent ($\nu = \nu_o'$) and a present ($\nu = \nu_o$) secondary wedge. To put it alternatively, the single mode supported by the structure will be activated in the same way regardless of the presence of the auxiliary component. Note that the permittivity in the corresponding region 1, ϵ_{r1}, is the same in the two cases.

[22] To elaborate further this point, we can consider a unitary homogeneous background field normal to the PEC plane written as: $\mathbf{E}_b = \mathbf{y}$ (in volt/meter). A modified quality factor $\mathcal{QF}^*$ could be defined as the ratio of the projection of the total field $\mathbf{E}_1$ (into the primary wedge) on the excitation field $\mathbf{E}_b$ in the presence of the secondary wedge, over the respective quantity in the absence of the secondary wedge. It is written in mathematical form as follows:

$$\mathcal{QF}^* = \frac{\iiint |\mathbf{E}_1^{(\nu_o)} \cdot \mathbf{E}_b| \mathrm{d}V}{\iiint |\mathbf{E}_1^{(\nu_o')} \cdot \mathbf{E}_b| \mathrm{d}V}. \tag{33}$$

In the following, it is shown that the alternative quality factor $\mathcal{QF}^*$ exhibits similar variations with the one based exclusively on modal solutions $\mathcal{QF}$, and thus, the latter quantity could be used as a field enhancement indicator even in the presence of external excitation.

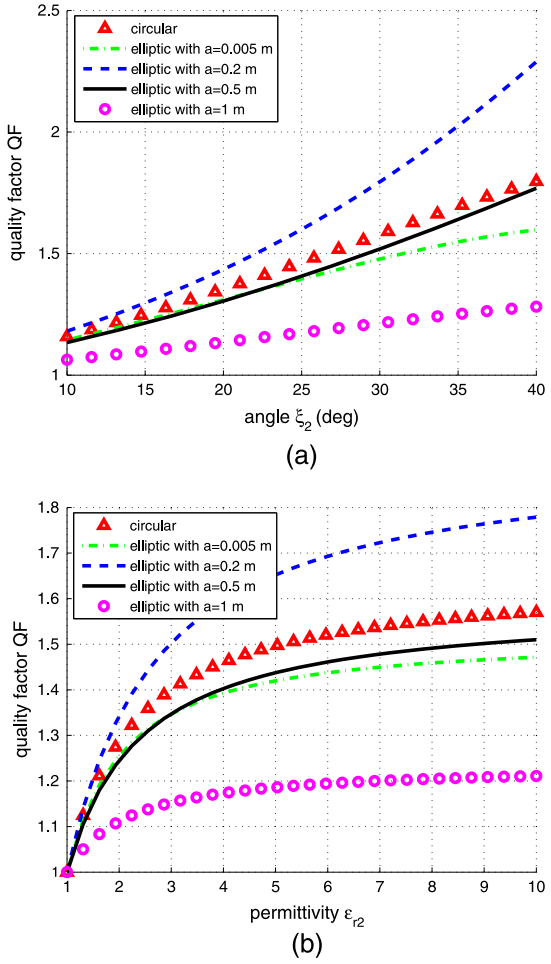

Figure 9. The quality factor $\mathcal{QF}$ as function of: (a) the secondary angle ξ_2 and (b) the angular extent ξ_2, for various distances a. Plot parameters: $\mu = 0.1$ rad/m, $\epsilon_{r1} = -0.5$, $\epsilon_{r2} = 2.5$, $R = 0.5$ m, $h = 1$ m, even case.

5.2. Exact Formulas ($\mu > 0$)

[23] In Figure 5a, we show the quality factor $\mathcal{QF}$ as function of the angular extent of the second wedge ξ_2 for various relative permittivities ϵ_{r2}, while the out-of-plane wave number μ is kept small ($\mu = 0.1$ rad/m). The behavior of all the curves is oscillatory, and the dependence from ξ_2 is stronger for electrically denser materials of the secondary component. The improvement in the field concentration across the primary wedge is not very significant even though it surpasses 50% in some cases. However, there are many zones where deteriorations ($\mathcal{QF} < 1$) in the measured quantity are recorded. In Figures 5b and 5c, where μ is slightly increased, the device performance is higher despite the fact that the waveform of the curves is similar. Finally, $\mathcal{QF}$ possesses much more substantial magnitudes when $\mu = 1$ rad/m as happening in Figure 5b.

[24] In Figure 6a, the quality factor $\mathcal{QF}$ is shown as function of the out-of-plane wave number μ for various angular extents ξ_2. One can clearly notice the upward sloping behavior curves at least when μ belongs to the considered interval $(0, 1)$. In case ξ_2 takes the two extreme values ($\xi_2 = \pi/6, \pi/3$), the quality performance experiences a drop for small μ which could be attributed to the asymmetry of the structure. In Figure 6b, where multiple ϵ_{r2} are regarded, we can notice again the beneficial influence of the out-of-plane wave number μ on the power concentration. It is remarkable that for $\epsilon_{r2} = 1.5, 3.5$, the improvement in the developed field along the metamaterial primary wedge is the same regardless of μ. The best choice for the dielectric permittivity is $\epsilon_{r2} = 4.5$; on the contrary, the performance of the auxiliary secondary structure is rather poor when $\epsilon_{r2} = 2.5$.

[25] In Figure 7, we use the same input parameters as in Figure 6, but the represented quantity is now the modified quality factor $\mathcal{QF}^*$ as defined in (33). By comparing Figure 7a with Figure 6a and Figure 7b with Figure 6b, one can clearly notice the similarity of the waveforms, even if the magnitude levels are different. Therefore, the ratio $\mathcal{QF}$ is not deprived of physical meaning, since almost the same variations are recorded when a background field $\mathbf{E}_b$ is assumed as taken into account in $\mathcal{QF}^*$.

5.3. Approximate Formulas ($\mu \to 0$)

[26] In Figure 8, we show the contour plots of the electric field magnitude $|\mathbf{E}| = \sqrt{|E_\rho|^2 + |E_\phi|^2 + |E_z|^2} = \sqrt{|E_u|^2 + |E_\theta|^2 + |E_z|^2}$ in decibel with respect to the geometrical coordinates into both the wedges for various cases. In Figures 8a and 8b, one can compare the electric power distribution in the absence and in the presence of a specific secondary volume. The assumption for slowly varying fields with respect to z is adopted, while the boundaries are marked with black color. It is obvious that the field into the auxiliary wedge is negligible compared to the vacuum case; in other words, the second volume "forces" the electric power to get concentrated externally to it. Note that possible discontinuities along the boundaries are anticipated since the represented quantity contains the discontinuous normal component. In Figures 8c and 8d, the same case is considered but for the hyperbolic-type configuration. The improvement in the intensity is more remarkable, again due to the very low field into the secondary component.

[27] In Figure 9a, the quality factor $\mathcal{QF}$ is shown as function of the angle ξ_2 for various elliptic coordinate systems with different focal distances a. It should be noted that an increasing ξ_2 contributes positively to the device effectiveness since the cross section of the auxiliary wedge, and accordingly, the low-field region of Figures 8b and 8d gets larger. Naturally, the curve corresponding to elliptic coordinates with small $a = 0.005$ m is close to that of the circular cylindrical configuration, while the optimal result is obtained for $a = 0.2$ m. With similar focal distances, one achieves better results than in the circular cylindrical case, a fact that is demonstrated by comparing Figure 8a with Figure 8b and Figure 9a with Figure 9b. In Figure 9b, where the independent variable is the secondary permittivity ϵ_{r2}, the curves are again increasing but with a slower pace than that of Figure 9). However, the choice of the focal distance affects similarly the structure effectiveness ($\mathcal{QF}$) in both the figures.

6. Conclusions

[28] Wedges with sharp or rounded edges are extensively utilized in modeling electromagnetic devices such as nanotips, probes, microscripts, and memory scanners. The effective operation of all these devices requires, for

different reasons each, an increased field concentration in the vicinity of the wedge's corner. For example, improved field intensity externally to the nanotip could be beneficial in electron microscope usage, while internal field enhancement is required in chemical experiments. In other words, whether we need high power concentrations into or outside the wedge is application-dependent; however, field enhancement close to the corner is always positively evaluated. In this work, we solve the electrostatic problem of a metamaterial wedge in the presence of a secondary dielectric wedge posed against the first one by forming a "bowtie" structure. Both circular and elliptic coordinate system configurations are introduced, while approximate expressions for slowly axially varying fields are obtained. A quality factor expressing the power enhancement has been defined and has been found to possess substantial magnitudes for certain angular extents and permittivities of the dielectric wedge. More specifically, it is found out that there is a clear increasing trend of this quality factor with the angle and the permittivity of the secondary wedge when the fields are weakly dependent on the axial coordinate. Furthermore, rapid oscillations are remarked when the geometrical variation along the axis gets stronger.

[29] An interesting expansion of the present study would be to insert multiple wedges around the primary metamaterial structure in order to achieve higher developed power into it. In this way, due to more degrees of freedom, a more realistic selection of parameters would be possible in order to render the device practically applicable. Furthermore, it would be intriguing to test the same configuration in the electrodynamic regime and observe if the beneficial amplifying properties hold.

[30] **Acknowledgments.** Dr. Valagiannopoulos acknowledges the Academy of Finland for postdoctoral project funding.

References

Abramowitz, M., and I. Stegun (1970), *Handbook of Mathematical Functions*, pp. 375–376, National Bureau of Standards, Washington, D. C.

Angulo, A. M., C. Noguez, and G. C. Schatz (2011), Electromagnetic field enhancement for wedge-shaped metal nanostructures, *J. Microelectromech. S.*, *2*, 1978–1983.

Aubry, A., D. Y. Lei, S. A. Maier, and J. B. Pendry (2010), Interaction between plasmonic nanoparticles revisited with transformation optics, *Phys. Rev. Lett.*, *105*, 233901.

Boardman, A. D., R. Garcia-Molina, A. Gras-Marti, and E. Louis (1985), Electrostatic edge modes of a hyperbolic dielectric wedge: Analytical solution, *Phys. Rev. B*, *32*, 6045–6047.

Davis, L. C. (1976), Electrostatic edge modes of a dielectric wedge, *Phys. Rev. B*, *14*, 5523–5525.

Dobrzynski, L., and A. A. Maradudin (1972), Electrostatic edge modes in a dielectric wedge, *Phys. Rev. B*, *6*, 3810–3815.

Gramotnev, D. K., D. F. P. Pile, M. W. Vogel, and X. Zhang (2007), Local electric field enhancement during nanofocusing of plasmons by a tapered gap, *Phys. Rev. B*, *75*, 035431.

Hassani, S. (2000), *Mathematical Methods: For Students of Physics and Related Fields*, pp. 436–437, Springer, New York.

Iwami, K., T. Ono, and M. Esashi (2006), Optical near-field probe integrated with self-aligned bow-tie antenna and electrostatic actuator for local field enhancement, *J. Microelectromech. S.*, *15*, 1201–1208.

Morse, P. M., and H. Feshbach (1953), *Methods of Theoretical Physics, Part I*, pp. 657–658, McGraw-Hill, New York.

Passian, A., R. H. Ritchie, A. L. Lereu, T. Thundat, and T. L. Ferrell (2005), Curvature effects in surface plasmon dispersion and coupling, *Phys. Rev. B*, *71*, 115425.

Pendry, J. B., A. Aubry, D. R. Smith, and S. A. Maier (2012), Transformation optics and subwavelength control of light, *Science*, *337*, 549–552.

Rockstuhl, C., C. R. Simovski, S. A. Tretyakov, and F. Lederer (2009), Metamaterial nanotips, *Appl. Phys. Lett.*, *94*, 113110.

Savage, K. J., M. M. Hawkeye, R. Esteban, A. G. Borisov, J. Aizpurua, and J. J. Baumberg (2012), Revealing the quantum regime in tunnelling plasmonics, *Nature*, *491*, 547–577.

Smythe, W. R. (1950), *Static and Dynamic Electricity*, Ch. 4, pp. 82–84, McGraw-Hill, New York.

Valagiannopoulos, C. A. (2009), On smoothening the singular field developed in the vicinity of metallic edges, *J. Appl. Electromag. Mechan.*, *31*, 67–77.

Vernon, K. C., D. K. Gramotnev, and D. F. P. Pile (2007), Adiabatic nanofocusing of plasmons by a sharp metal wedge on a dielectric substrate, *J. Appl. Phys.*, *101*, 104312.

Vinogradov, S. S., P. D. Smith, and E. D. Vinogradova (2001), *Canonical Problems in Scattering and Potential Theory*, 392 pp., CRC Press, Washington.

Wallen, H., H. Kettunen, and A. Sihvola (2008), Surface modes of negative-parameter interfaces and the importance of rounding sharp corners, *Metamaterials*, *2*, 113–121.

Zayats, A. V., I. I. Smolyaninov, and A. A. Maradudin (2005), Nano-optics of surface plasmon polaritons, *Phys. Rep.*, *408*, 131–314.

Zeng, Y., J. Liu, and D. H. Werner (2011), General properties of two-dimensional conformal transformations in electrostatics, *Op. Express*, *19*, 20035–20047.

Zhang, X., and Z. Liu (2008), Superlenses to overcome the diffraction limit, *Nat. Mat.*, *7*, 435–441.